output power in the 60-GHz range. The results achieved with the module have demonstrated the feasibility of an all-solid-state millimeter-wave transmitter module capable of a data rate greater than 1 Gbit/s. The output power may further be increased by means of combining a larger number of diodes and the use of double-drift IMPATT diodes capable of higher output power [14].

REFERENCES

[1] W. J. Clemetson, N. D. Kenyon, K. Kurokawa, B. Owen, and W. O. Schlosser, "An experimental mm-wave path length modulator," *Bell Syst. Tech. J.*, vol. 50, pp. 2917–2945, Nov. 1971.

[2] H. J. Kuno, "Analysis of nonlinear characteristics and transient response of IMPATT amplifiers," *IEEE Trans. Microwave Theory Tech. (Special Issue on Solid-State Microwave Power Amplifiers)*, vol. MTT-21, pp. 694–702, Nov. 1973.

[3] H. J. Kuno and D. L. English, "Nonlinear and large-signal characteristics of millimeter-wave IMPATT amplifiers," *IEEE Trans. Microwave Theory Tech. (Special Issue on Solid-State Microwave Power Amplifiers)*, vol. MTT-21, pp. 703–706, Nov. 1973.

[4] H. J. Kuno, "Analysis and characteristics of *P-N* junction diode switching," *IEEE Trans. Electron Devices*, vol. ED-11, pp. 8–14, Jan. 1964.

[5] W. O. Schlosser and K. Kurokawa, "Insertion loss of 4-level phase switch," *IEEE Trans. Microwave Theory Tech.* (Short Papers), vol. MTT-20, pp. 614–616, Sept. 1972.

[6] S. Stein and J. J. Jones, *Modern Communication Principles*. New York: McGraw-Hill, 1967.

[7] K. Kurokawa and W. O. Schlosser, "Quality factor of switching diodes for digital modulation," *Proc. IEEE* (Lett.), vol. 58, pp. 180–181, Jan. 1970.

[8] W. Bennett and R. Davy, *Data Transmission*. New York: McGraw-Hill, 1965.

[9] H. J. Kuno, D. L. English, and P. H. Pusateri, "Millimeter-wave solid state exciter-modulator-amplifier module for gigabit data rate," presented at the 1972 IEEE Int. Microwave Symp., Chicago, Ill., May 1972.

[10] Y. Fukatsu, M. Akaike, and H. Kato, "Amplification of high speed PCM phase-shift keyed millimeter-wave signals through an injection locked IMPATT oscillator," presented at the 1971 Int. Solid State Circuits Conf., Philadelphia, Pa., Feb. 1971.

[11] Y. Chang, D. L. English, and H. J. Kuno, "Four gigabits per second millimeter-wave exciter-modulator-amplifier module," presented at the 1974 IEEE Int. Microwave Symp., Atlanta, Ga., June 1974.

[12] H. J. Kuno, K. P. Weller, and D. L. English, "Tunable millimeter-wave packaged IMPATT diode oscillator," presented at the 1974 IEEE Int. Microwave Symp., Atlanta, Ga., June 1974.

[13] H. J. Kuno, D. L. English, and R. S. Ying, "High power millimeter-wave IMPATT amplifiers," presented at the 1973 IEEE Int. Solid-State Circuit Conf., Philadelphia, Pa., Feb. 1973.

[14] H. J. Kuno and D. L. English, "Microwave power combinatorial development—60 GHz amplifier/combiner," Tech. Rep. AFAL-TR-73-355, 1974.

[15] H. J. Kuno, Y. Chang, and D. L. English, "Millimeter-wave PSK transmitter module," Tech. Rep. AFAL-TR-74-175, 1974.

Frequency Multiplication by a P-I-N Diode When Driven into Avalanche Breakdown

PASTEUR L. NTAKE, STUDENT MEMBER, IEEE, AND D. R. CONN, MEMBER, IEEE

Abstract—**An investigation of frequency multiplication using a step-recovery diode (SRD) driven into avalanche breakdown is presented. This mode of operation, which is called the "breakdown mode," consists of a reverse-biased p-n junction, SRD, or IMPATT diode driven into reverse breakdown by an ac signal source. As the diode voltage passes from reverse bias to reverse breakdown and avalanche, the state of the diode switches quickly from a depletion-layer capacitance to an avalanche inductance; hence the production of strong harmonics. A theoretical analysis and experimental investigation of a coaxial/waveguide 2–6-GHz frequency multiplier using HP5082-0320 step-recovery diodes, [R_S = 0.75 Ω, C_d(-6v) = 1.0 pF] shows that the breakdown-mode frequency multiplier has a higher conversion efficiency than the conventional "charge-storage" multiplier. A measured conversion efficiency of 73 percent was achieved while the *same circuit* configuration produced 52 percent for the *same* diode used as a charge-storage multiplier under optimum forward-drive and tuning conditions. Also the theory developed in this paper indicates a maximum possible conversion efficiency of 80 percent for the breakdown-mode multiplier, which corresponds closely with the measured results, and a maximum theoretical efficiency for a forward-driven diode of 64 percent. The performance of an FM microwave system was monitored using the breakdown multiplier as a LO in which a baseband SNR of 59 dB was recorded.**

Manuscript received August 27, 1974; revised January 27, 1975. This research was jointly supported by Carleton University and by National Research Council Grant N.R.C. 2056-87-A8447.

The authors are with the Faculty of Engineering, Carleton University, Ottawa, Ont., Canada.

I. INTRODUCTION

VARACTOR frequency multipliers have progressed from the work of Penfield and Rafuse [1] with nominally driven abrupt junction-diodes to the general analysis and design of varactor frequency multipliers with the arbitrary capacitance variation and drive level by Burckhardt [2], Scanlan [3], and others.

The overdriven stored-charge multiplier is characterized by high efficiency, decreasing with the order of multiplica-

tion, low I^2R losses, and hence high-power output capability, which is limited eventually by the diode breakdown voltage and thermal resistance. Also there is little added FM or AM noise to the carrier [4] for a correctly designed and tuned circuit.

This paper, on the other hand, presents an investigation of a step-recovery diode (SRD), which is used as a frequency multiplier by driving it from a reverse-bias displacement-current state into avalanche breakdown. As the diode passes from reverse bias to breakdown it quickly switches impedance levels from a small depletion-layer capacitance to a small avalanche inductance. That is, it switches from a *large* capacitive impedance to a *small* inductive impedance. With the conventional SRD frequency multiplier the diode switches from a large capacitive impedance in reverse bias to a small capacitive impedance in forward bias. This fundamental difference in the switching method led us to the study presented in this paper, expecting heuristically that the switching discontinuity would be greater in the breakdown case.

A comparison of the forward-driven SRD frequency multiplier with the reverse-driven SRD frequency multiplier is implemented by constructing a single-frequency multiplier coaxial/waveguide circuit (Fig. 1) used for both methods of multiplication and using identical diodes for the tests. In each test the circuit was optimally tuned and biased. Hence, in this way, the circuit losses and diode series resistance were approximately the same for the comparison.

The analysis presented in this paper applies the method given by Burckhardt and Scanlan to the case of overdrive in the reverse-avalanche region. This analysis is general in the sense that it includes the following modes of operation:

1) conventional varactor—no overdrive;
2) forward-driven varactor—stored charge;
3) reverse-driven varactor—avalanche breakdown;

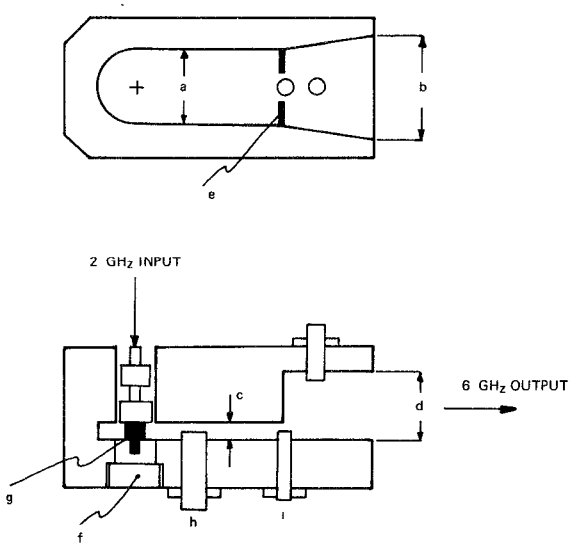

Fig. 1. 6-GHz stored-charge and breakdown-frequency multiplier. Legend: a = 28.5 mm; b = 33.8 mm; c = 2.28 mm; d = 15.8 mm; fc = 5.3 GHz.

4) reverse *and* forward overdrive.

The present analysis follows that of Burckhardt's in most respects. That is, circuit losses are ignored while diode losses are accounted for through a fixed series resistance R_s. Also it is assumed that all the input power is converted to one single output frequency and no idler currents flow in the diode or external circuits.

II. DIODE MODEL AND ASSUMPTIONS

The diodes used in this investigation are SRD (p-i-n diodes). Hence the varactor model chosen for the analysis is essentially the same as that used by Burckhardt, in which the diode is represented by a depletion-layer capacitance in series with a constant resistance R_s for applied voltages between reverse breakdown and the contact potential Φ, and it is assumed that for forward bias the voltage remains clamped at the contact potential Φ, with the charge varying. Hence in the forward region the capacitance becomes infinite. The model, then, ignores recombination of minority carriers during forward conduction, an approximation which is valid if the recombination time for minority carriers is much greater than the period of oscillation.

For the reverse-biased region the diode voltage is given by [5].

$$V_d(Q) = \Phi - (V_{Br} + \Phi)\left(\frac{Q}{Q_{Br}}\right)^{\gamma}, \qquad |V_d| < |B_{Br}| \quad (1)$$

where

$|V_{Br}|$ the breakdown voltage, absolute value;
Φ contact potential;
Q stored charge;
γ a constant;
= 2, for an abrupt junction-diode;
$\simeq$ 1, for a SRD.

For the reverse-breakdown region the modeling is not as straightforward. The IMPATT-diode theories of Read [6], Hines [7], and Misawa [8] show that the process of, avalanche leads to nonlinear differential equations which, under suitable conditions, can be linearized to produce small-signal models consisting of a resonant circuit containing an avalanche inductance L_a, a capacitance C_d, and negative conductance G_a. In the present study, the output frequency was much less than the avalanche resonant frequency (see Appendix I), which resulted in the avalanche conduction current through L_a dominating the displacement current and negative-conductance current. For this analysis, it has been assumed that the avalanche inductance is a constant, and hence that the avalanche current increases linearly with time for a fixed applied voltage. Because of this linearization, the theory presented can only be expected to predict the performance of this type of frequency multiplier for small amounts of reverse overdrive, <0.4. The limitation of this constant avalanche inductance was explored by a close comparison of the experimental results with theory and is presented

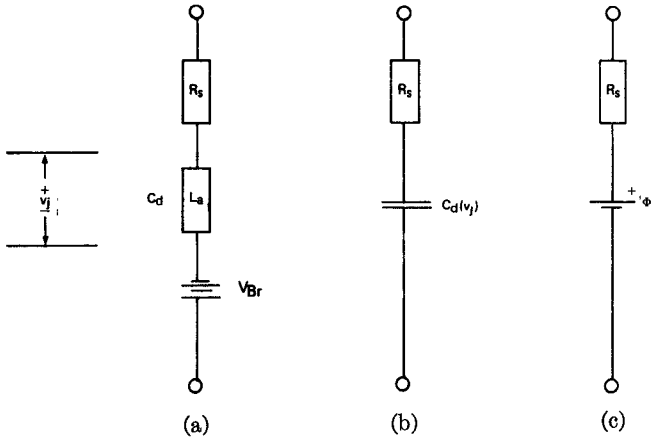

Fig. 2. Diode circuit model for (a) avalanche-, (b) reverse-, and (c) forward-bias regions.

in Section V. For the present study the avalanche inductance is given by [8] as

$$L_a = \frac{W}{v_s} = \frac{1}{3\alpha' I_0} \tag{2}$$

where W is the width of the avalanche region, v_s is the saturated carrier velocity, α' is the derivative of the ionization coefficient α with respect to electric field, and $|I_0|$ is the diode dc current. For other structures, such as p-n IMPATT diodes, (2) must be modified [9].

The complete circuit model for the three regions of operation then is given in Fig. 2, with the diode parameters and constants summarized in Appendix I.

III. ANALYSIS

The analysis begins by assuming that the following conditions are met.

1) The power is dissipated in the load only at the desired frequency and only fundamental power is dissipated in the source.

2) The source is conjugately matched at the fundamental frequency.

3) Circuit losses are not considered. The diode series resistance is approximated by a constant R_S.

4) The diode dc current is not contained in the analysis, and hence dc power dissipation is not calculated. This assumption was also used by Burckhardt [2] and limits the useful results to small forward or reverse overdrive.

5) A shunt-connected multiplier circuit (Fig. 3) is analyzed with circulating currents i_1 and i_n flowing in the input and output loops, respectively.

A. Diode Analysis—AC

In this analysis only ac currents are considered; hence there is no prediction of dc power consumption or dc-to-RF efficiency. It is assumed, however, that the total charge flowing into the diode consists of a dc term Q_0 plus two time-varying harmonic terms. The term Q_0 is retained only to set a proper bias voltage and to allow consistent definitions of forward and reverse overdrive which follow directly from Burckhardt. The assumption of zero dc current is equivalent to the separate assumptions of infinite carrier lifetime in the forward-biased region and the reverse-biased region. These assumptions, along with a fixed avalanche inductance, limit the accuracy of the results for the cases of large overdrive.

Consider the diode driven by two harmonically related charges (Fig. 4) given by

$$Q(t) = Q_0 + Q_1 \cos \omega t + Q_n \cos (n\omega t + \phi_n) \tag{3}$$

where Q_0, Q_1, Q_n are the average, fundamental, and nth harmonic-charge amplitudes, respectively; ω is the input frequency; and ϕ_n is the phase angle of the nth harmonic charge.

Equation (3) can be written as

$$Q(t) = Q_0 + Q_1 K \tag{4}$$

where

$$K = \cos \omega t + R_n \cos (n\omega t + \phi_n) \tag{5}$$

and

$$R_n = Q_n / Q_1 \tag{6}$$

is the charge ratio.

Using the same technique as Burckhardt, the maximum and minimum charges $Q_{\max}$,$Q_{\min}$ can be defined in terms of forward- and reverse-overdrive coefficients in the

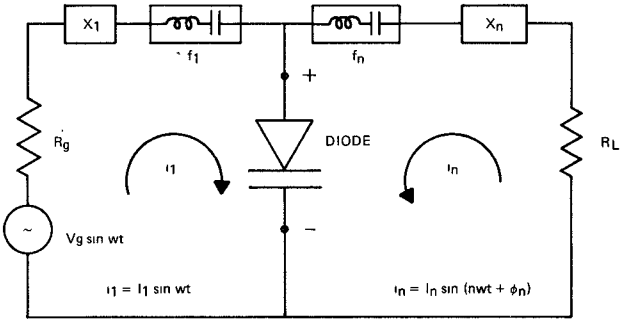

Fig. 3. The idlerless shunt-connected multiplier circuit.

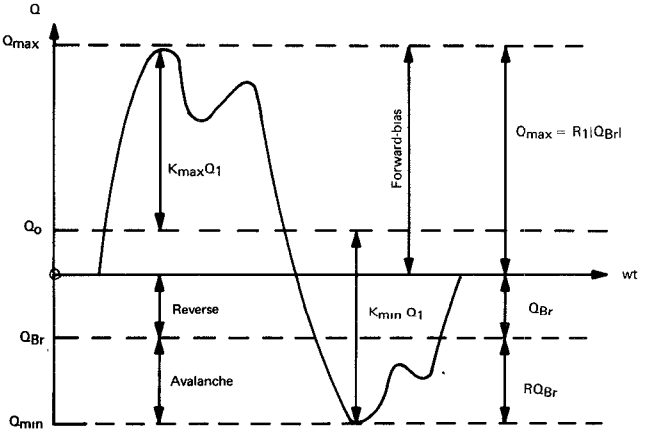

Fig. 4. The applied-charge waveform (typical function).

following manner: Q_{max} and Q_{min} are defined as

$$Q_{max} \triangleq R_f \mid Q_{Br} \mid \tag{7}$$

for forward overdrive and

$$Q_{min} \triangleq (1 + R_r) Q_{Br} \tag{8}$$

for reverse overdrive, where Q_{Br} is the charge stored in the diode at reverse breakdown with R_f and R_r representing the forward- and reverse-overdrive coefficients, respectively. As seen from the definition of R_r, a reverse overdrive of zero represents a diode driven to, but not past, avalanche breakdown, while forward overdrive of zero represents a diode driven to, but not past, zero bias. The charge coefficients Q_0, Q_1, Q_n, and K are related to the drive coefficients by the following:

$$Q_0 = \mid Q_{Br} \mid \left[R_f - \left(\frac{K_{max}}{K_{max} - K_{min}} \right) (1 + R_f + R_r) \right] \tag{9}$$

$$Q_1 = \mid Q_{Br} \mid (1 + R_f + R_r)/(K_{max} - K_{min}) \tag{10}$$

and

$$Q_n = R_n Q_1 \tag{11}$$

where K_{max} and K_{min} are the maximum and minimum values of K.

For example, consider the special case of $R_f = R_r = 0$, $n = 3$, and $R_n = 1$, with $\phi_n = 0$. Then $K_{max} = 2$, $K_{min} = -2$, and $Q_0 = - \mid Q_{Br} \mid /2$, $Q_1 = \mid Q_{Br} \mid /4$, and $Q_n = \mid Q_{Br} \mid /4$, which shows that the diode is biased at half the breakdown charge with Q_1 and Q_n being equal to $(Q_{Br}/4)$. Hence, from (4), $Q_{max} = 0$ and $Q_{min} = - \mid Q_{Br} \mid$, which indicates a fully driven varactor multiplier.

The diode terminal voltage $V_d(t)$ is given by

$$V_d(t) = \begin{cases} R_S i_d(t) + \Phi, & Q > 0 \\ R_S i_d(t) + \Phi - (V_{Br} + \Phi)(Q/Q_{Br})^{\gamma}, & Q_{Br} < Q < 0 \\ R_S i_d(t) - V_{Br} + L_a (di_d/dt), & Q < Q_{Br} \end{cases} \tag{12}$$

where

i_d	diode current;
R_S	fixed-series bulk resistance of the diode;
Φ	diode contact potential;
Q_{Br}	diode charge at breakdown;
γ	$= 1/(1 - m)$;
m	$= 1/2$, for abrupt junction-diode;
	$= 1/3$, for a linearly graded diode;
L_a	avalanche inductance;
V_{Br}	breakdown voltage.

The diode current is given by

$$i_d(t) = \frac{dQ}{dt} = I_1 \sin \omega t + I_n \sin (n\omega t + \phi_n). \tag{13}$$

Given the diode charge and current coefficients at the fundamental and nth harmonic, it only remains to find the fundamental and nth harmonic voltage from (4) and (5). This is accomplished in a straightforward manner by expressing $V_d(t)$ as a Fourier series. That is

$$V_d(t) = A_0/2 + \sum_{n=1}^{N} (A_N^2 + B_n^2)^{1/2} \sin (n\omega t + \phi_n)$$

where the coefficients A_0, A_n, B_n, ϕ_n are evaluated by the usual method of Fourier series.

B. Circuit Analysis

The circuit analysis (Fig. 3), for the shunt-mounted frequency multiplier follows the method outlined by Scanlan [3]. Hence only the results are presented in this paper. These are

$$R_{IN} = B_1 \mid I_1$$

$$X_{IN} = - A_1 \mid I_1$$

$$R_L = -(A_N \sin \phi_n + B_n \cos \phi_n)/I_n$$

$$X_L = -(A_N \cos \phi_n - B_n \sin \phi_n)/I_n$$

$$P_{IN} = I_1^2 R_{IN}/2$$

$$P_{OUT} = I_n^2 R_L/2$$

$$\eta = \frac{P_{OUT}}{P_{IN}} = (I_n/I_1)^2 R_L/R_{IN}$$

where

R_{IN}	the input resistance;
X_{IN}	the input reactance;
R_L, X_L	the load resistance and reactance, respectively;
P_{IN}	the input power at the fundamental;
P_{OUT}	the output power at the nth harmonic;
η	the efficiency.

The numerical method of solution is summarized in Appendix II.

IV. EXPERIMENTAL METHOD

A. 6-GHz Multiplier Circuit $n = 3$

A sketch of the frequency multiplier used for this investigation is shown in Fig. 1. As can be seen, this circuit is a conventional design using a coaxial low-pass filter/transformer on the input with the diode shunt mounted across a reduced-height rectangular waveguide on the output. The cutoff frequency, 5.3 GHz, of the waveguide is designed to attenuate all of the lower frequencies, 2 and 4 GHz.

B. Measurement Systems

The basic multiplier measurement system is given in Fig. 5, and the system used to measure FM noise is given in Fig. 6. The basic measurement system was designed to insure that all critical components such as the TWT amplifier were properly terminated and that no unwanted harmonically related signals appeared on the input or output as monitored on an AIL-707 spectrum analyzer.

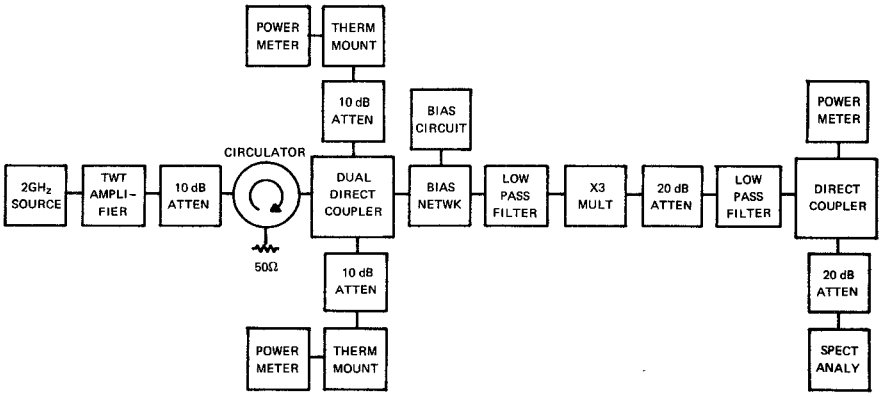

Fig. 5. Block diagram of basic experimental apparatus.

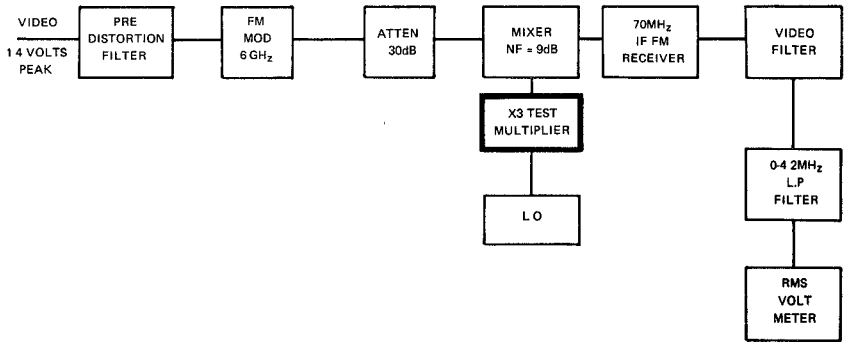

Fig. 6. Block diagram of noise-measurement set.

In fact, all unwanted signals which could influence power measurements were at least 35 dB below the output power at 6 GHz. This was accomplished (see Fig. 5) by the use of low-pass filters on the input and output of the multiplier, as well as using a 5.3-GHz cutoff for the multiplier waveguide. Higher frequencies such as 8 and 10 GHz were effectively terminated by the frequency-multiplier output cavity.

The measurement system (Fig. 6) which was chosen to evaluate the FM noise contribution of this breakdown multiplier to a communication system is a conventional FM microwave link with predistortion [10]. The system was designed for color TV with a baseband bandwidth of 4.2 MHz and a peak carrier deviation of 4 MHz produced by a 1.4-V video signal. With this system it is possible to measure the peak signal to rms noise in a 4.2-MHz band and compare this with the usual system requirements [10] for color TV.

Of course, the more direct and difficult approach is to construct a microwave bridge such as Ondria's [11] with which the fine structure of FM noise can be studied. This method was not chosen for this initial noise study since a microwave link was available and because the microwave link measurements relate directly to a common system requirement, i.e., SNR in color TV.

C. Tuning and Biasing of the Breakdown Multiplier

It was found that the breakdown mode is particularly stable, i.e., no unwanted oscillations when driven from a constant-current source. This mode is, of course, characterized by a large reverse current, 25 mA in this case, which is much less in the charge-storage multiplier. It is in this way that the mode of operation is identified, as well as by observing the large difference in operating dc voltages.

The tuning on the input is fixed for a given transformer, but can be easily changed by inserting different low-pass filter/transformer structures. The output tuning is accomplished by tuning screws (Fig. 1).

V. RESULTS

A. Theoretical: $n = 3, f_0 = 6$ GHz

The results of the previous sections are presented in Figs. 7 and 8 where input resistance and efficiency are plotted as contours on an overdrive-load resistance plane for an overdriven charge-storage multiplier and an overdriven breakdown multiplier. The R_f,R_L plane for the overdriven stored-charge multiplier indicates a maximum efficiency of 64 percent, with an input resistance of 2.8 Ω and an output resistance of 4.4 Ω.

Similarly, the contours of input resistance and efficiency of the breakdown-mode multiplier biased at 25 mA (Fig. 8) show that the efficiency is maximized 80 percent at an input resistance of 4.6 Ω and a load resistance of 7.6 Ω. Thus the breakdown-mode multiplier shows greater input/output resistance levels than the conventional overdriven charge-storage multiples for the particular case.

Notice from Fig. 8 that a very small overdrive, <0.1,

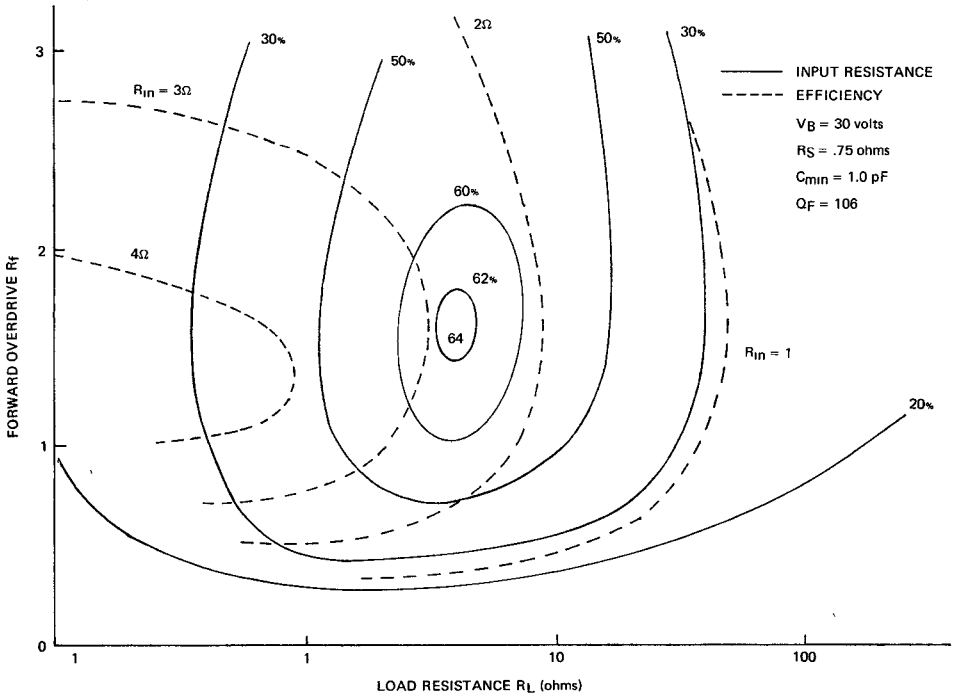

Fig. 7. Efficiency and input resistance contours of the stored-charge multipliers. $R_f \neq 0$; $R_r = 0$.

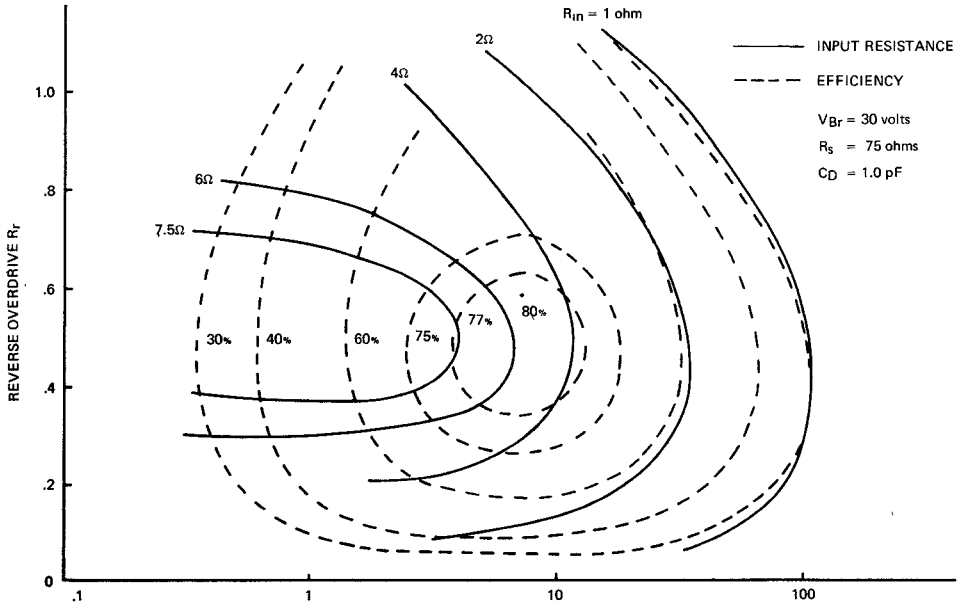

Fig. 8. Efficiency and input resistance contours of the breakdown multiplier. $R_f = 0$; $R_r \neq 0$.

yields a relatively high effiiciency of 40 percent, a point to be considered when trading off efficiency and FM noise.

B. Experimental: $n = 3, f_0 = 6$ GHz

The experimental results for the two types of multiplier circuits are presented in Figs. 9 and 10.

Fig. 9 shows a plot of output power versus bias current for the breakdown-mode multiplier with the input power held constant at 500 mW. It is seen that the optimum bias current is approximately 25 mA and that this value is somewhat dependant on C_d.

In Fig. 10 the optimum experimental curves of n versus input power are compared with the theoretical values for both the forward-driven multiplier and the reverse driven. It is seen that for the forward-driven multiplier, experiment and theory agree well for input power levels between 300 and 1300 mW, while they diverge for low levels. On the other hand, for the case of the breakdown multiplier, the theory (using the piecewise-linear model) agrees well with experiment for low power levels up to about 500 mW. Above 500 mW the theory predicts almost constant efficiency, while the experiments show progressively decreas-

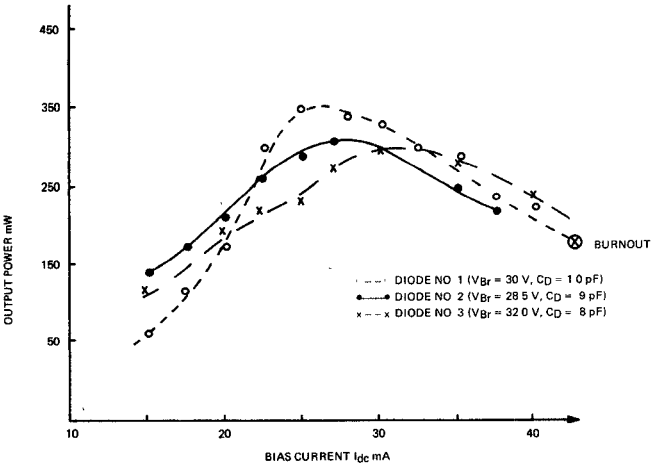

Fig. 9. Output power versus bias current for breakdown multiplier. P_{IN} = 500 mW.

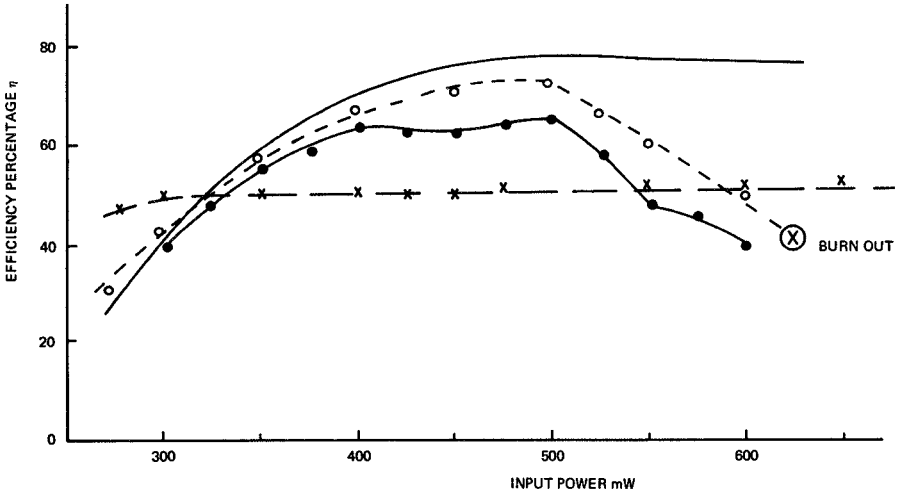

Fig. 10. Efficiency versus input power for both types of multipliers. Legend: ———— Theory (breakdown mode) R_L = 11.5 Ω. o–o–o–o– Experimental—breakdown mode, diode 1. •–•–•–•– Experimental—breakdown mode, diode 2. x–x–x–x– Experimental—stored charge, diode 2.

ing efficiency as the input power is increased. It was also noted that large variations in L_a in the analysis had little effect on the efficiency indicating the need for a much more complex theory for very large reverse overdrive.

For a bias current of 25 mA and output power of 300 mW (tuned for maximum efficiency) the noise power in a 4.2-MHz baseband was 59 dB below the peak signal (1.4 V in a 75-Ω video system). Although a detailed noise study of the complete system has not been undertaken it is reasonable to assume that the breakdown multiplier is the major source of FM noise in the system. For example, the SNR at baseband is given by [10]

$$\text{SNR} = 3P_c\beta^2/KTf_1n_f$$

where

β	modulation index $\simeq$1 for this system;
KT	$= -174$ dB$_m$/Hz;
n_f	noise factor of mixer;
f_1	maximum baseband frequency (4.2 MHz);
P_c	carrier power (-10 dB$_m$);

giving an expected SNR of 94.6 dB, which is much greater than the measured results.

The total rms frequency deviation of the carrier in a 4.2-MHz band can be calculated [10] from the measurements of baseband noise and signal power. That is

$$P_s/P_n = \Delta f_s^2/\overline{\Delta f_n^2}f_1 = \text{SNR}$$

where

P_s	peak signal power detected at frequency f_1, 4.2 MHz;
P_n	total baseband noise power;
Δf_s	peak carrier-frequency deviation due to the modulating signal;
$\overline{\Delta f_n^2}$	mean square-frequency deviation of the carrier due to noise per hertz of bandwidth;
SNR	baseband peak signal-to-rms-noise ratio.

In this case, SNR = $10^6/1.26$, f_1 = 4.2 MHz, and Δf_s = 4 MHz.

Hence, $\Delta f_n^2 = 4.8$, $\Delta f_{n,\text{rms}} = 2.2$ Hz, which is more than a cavity-stabilized [12] IMPATT-diode oscillator, but much less than a low-Q unstabilized IMPATT-diode oscillator.

VI. SUMMARY AND CONCLUSIONS

The possibility of frequency multiplication by driving a p-i-n diode into avalanche breakdown has been demonstrated theoretically with a simple piecewise-linear model of a p-i-n diode and confirmed experimentally. The theoretical and experimental results show that higher conversion efficiencies can be obtained by driving the varactor into the avalanche region than by driving it into forward conduction.

The theory predicted a maximum conversion efficiency of 80 percent, while 73 percent was achieved. For the same diode the stored-charge multiplier theory predicts 64-percent efficiency, while 50 percent was achieved. Also, as would be expected because of the large dc power dissipation in the breakdown multiplier, its maximum output power is less than the stored-charge multiplier.

It has been shown experimentally that the diode modeled in the reverse-breakdown region as a small fixed inductance in parallel with a capacitance is valid for reverse overdrive of approximately 0.4 ($\approx$500 mW of input power), while the computations show that the calculations of efficiency are not significantly dependent on L_a over rather large variations of that parameter. Hence no attempt has been made at this point to extend the diode modeling into a complete nonlinear characterization. Modeling the diode as a fixed small inductance in breakdown, then, is equivalent to the forward-region approximation where $C_D \rightarrow \infty$. That is, both regions act as an energy-storage mechanism with small ac voltages developed.

The FM noise properties of the breakdown multiplier have been investigated by observing the SNR in a microwave link designed for video transmission. A SNR of 59 dB was achieved at baseband, while a high-quality video transmission system requires [10] approximately 55 dB for essentially transparent signal transmission

This preliminary test therefore suggests further investigations should be performed in the area of FM noise in order to optimize the circuit design and minimize the noise.

While the numerical method employed in this investigation was satisfactory and accurate, the method should be extended to include an optimization routine which will lead to shorter computing times or give the possibility of evaluating more complex diode models and circuits.

Further comparisons of the two methods of multiplication are presented in Table I.

As further extensions of this work, it is proposed to investigate the IMPATT diode as a multiplier with the aim of exploiting its negative-resistance capabilities at higher frequencies and to perform experiments with Gunn diodes biased below threshold.

TABLE I

	STORED CHARGE Multiplier	BREAKDOWN Multiplier ($n = 3$, $F_o = 6\text{GH}_z$)
P_o	840mw	500
η	52%	73%
f-m noise	low	high
Bandwidth	5%	7%
Impedance levels	low	higher
TEMP	Relatively insensitive	η falls off with higher temp.
dc power consumption	~ 0	750mw
parasitic oscillation	critical to tune	insensitive when biased from constant current source
I_o	<2mA	25mA
η(dc-rf)	52%	~40%

APPENDIX I

DIODE PARAMETERS

The average properties of the devices used in this test are summarized in Table II, from which the avalanche inductance, conductance, and susceptance can be calculated [8]. Specifically, $L_a = \tau_a/3\alpha' I_0 = 0.27$ nH at 25 mA; X_a at 6 GHz $= 10.2\,\Omega$ (0.1 mho); $G_a = \alpha' I_0/5 = 2$ mmho; $B_d = \omega C_d = 38$ mmho at 6 GHz, at 30 V; and $f_a^2 = 1/2\pi L_a C_a = 9$ GHz.

From these calculations it is seen that the avalanche inductance L_a dominates the conductance and capacitance for the frequency range in question; i.e., $f_0 < 9$ GHz, the avalanche resonant frequency of these diodes.

APPENDIX II

NUMERICAL METHOD

This appendix outlines the numerical method used in the analysis of this multiplier. The essential steps followed in order are as follows.

1) The initial values of the charge-waveform parameters R_f, R_r, ϕ_n, and R_n are assigned.

2) The diode parameters V_{Br}, R_s, m, C_0, and W are assigned, as well as the assumed diode current I_0 and n the order of multiplication.

3) The diode's avalanche inductance is computed.

4) Using the overdrive values R_f and R_r with the phase angle ϕ_n, the diode voltage $V_d(t)$ is calculated.

5) The fundamental Fourier coefficients A_1 and B_1, and the nth harmonic coefficients A_n and B_n of the diode volage waveform are computed from a fast Fourier transform algorithm [13].

6) Impedance levels, input and output powers, and nth

TABLE II

Parameter	Symbol	Source of data	Value
Breakdown voltage	V_{Br}	Static I-V measurement	30 volts
Depletion layer capacitance	C_{mn}	C-V measurement	1.0pF
Intrinsic layer width	W	breakdown measurements (10)	0.8μm
Derivative of ionization rate	α^1	(8)	0.405 $volt^{-1}$
Saturated velocity	V_s	(8)	10^7cm/sec
dc current	I_o	external bias measurement	25mA
avalanche transit time	τ_a	W/V_s	8PS

harmonic-voltage phase angle θ_n are calculated for the given set of input parameters.

7) The output-charge phase angle ϕ_n is varied between $-3\pi/2$ and $3\pi/2$ in increments until maximum conversion efficiency is obtained.

8) The charge ratio R_n is now varied in small steps to simulate a varying R_L and steps 4)–7) are repeated.

9) The overdrive coefficients are varied corresponding to the mode of operation under study and the previous steps are repeated.

REFERENCES

[1] P. Penfield and R. P. Rafuse, *Varactor Applications*. Cambridge, Mass.: M.I.T. Press, 1962.

[2] C. B. Burckhardt, "Analysis of varactor frequency multipliers for arbitrary capacitance variation and drive level," *Bell Syst. Tech. J.*, vol. 44, pp. 675–692, 1966.

[3] I. O. Scanlan, "Analysis of varactor harmonic generators," *Advan. Microwaves*, vol. 2, pp. 115–236, 1967.

[4] "Harmonic generation using step recovery diodes and SRD modules," Hewlett-Packard, Application Note 920, p. 25.

[5] W. Shockley, "The theory of p-n junctions in semiconductors and p-n junction transistors," *Bell Syst. Tech. J.*, vol. 28, p. 435, 1949.

[6] W. T. Read, "A proposed high-frequency negative-resistance diode," *Bell Syst. Tech. J.*, vol. 37, pp. 401–446, 1958.

[7] M. E. Hines, "Noise theory for Read type avalanche diode," *IEEE Trans. Electron Devices (Special Issue on Semiconductor Bulk-Effect and Transit-Time Devices)*, vol. ED-13, pp. 158–163, Jan. 1966.

[8] T. Misawa, "Negative resistance in *p-n* junctions under avalanche breakdown condition, Part I," *IEEE Trans. Electron Devices (Special Issue on Semiconductor Bulk-Effect and Transit-Time Devices)*, vol. ED-13, pp. 137–143, Jan. 1966.
——, "Negative resistance in *p-n* junctions under avalanche breakdown condition, Part II," *ibid.*, vol. ED-13, pp. 143–151, Jan. 1966.

[9] H. A. Watson, *Microwave Semiconductor Devices and Their Circuit Application*. New York: McGraw-Hill, 1969.

[10] *Transmission Systems for Communications*, 4th ed., Bell Telephone Labs., Feb. 1970.

[11] J. G. Ondria, "A microwave system for measurement of AM and FM noise spectra," *IEEE Trans. Microwave Theory Tech. (Special Issue on Noise)*, vol. MTT-16, pp. 767–781, Sept. 1968.

[12] J. R. Ashley and C. B. Searles, "Microwave oscillator noise reduction by a transmission stabilizing cavity," *IEEE Trans. Microwave Theory Tech. (Special Issue on Noise)*, vol. MTT-16, pp. 743–748, Sept. 1968.

[13] J. W. Cooley, P. A. W. Lewis, and P. D. Welch, "The fast Fourier transform and its applications," *IEEE Trans. Educ.*, vol. 12, pp. 27–34, Mar. 1969.